

## Multiresolution Analysis of Heart Sounds Using Filter Banks

B. El-Asir and K. Mayyas

Department of Electrical Engineering, Jordan University of Science and Technology, Jordan

**Abstract:** Discrete wavelet analysis can efficiently be implemented by filter banks. This paper studies heart sound signals using a wavelet filter banks structure. The heart sound signals are viewed into different wavelet subspaces by expanding them uniquely into sub-band signals of varying time-frequency resolutions. This provides the ability to isolate and distinguish different vital time-frequency information from the original heart sound signal and to explore the physical characteristics of heart sounds and murmurs such as the presence of opening snap, third and fourth heart sounds, auscultatory gap, high and low frequency systolic and diastolic murmurs. Very specific important features can be extracted from this information and used as a base for an informative diagnostic tool to classify heart diseases. Preliminary results show the significance of this technique in emphasizing the diagnostic information obtainable from auscultation and in helping to bring cardiac auscultation into prominence again along with more modern technologies such as scans, echo and Doppler scans. These results are believed to be satisfactory and promising

**Key words:** Auscultation, classification, heart sounds, informative, multi-resolution, murmurs, phonocardiograph, wavelets

### INTRODUCTION

Frequency contents of heart beat sounds and their time locations in the cardiac cycle are among the most important characteristics which aid the detection of murmurs. Murmurs are described by noisy fluctuations with high frequencies, up to 600 Hz and are correlated with heart beat diseases. FFT analysis has been used in various studies to determine the frequency components of heart sounds<sup>[1]</sup>. FFT analysis remains of limited value, because heart sound signals are non stationary signals. The discrete Wigner distribution method<sup>[2]</sup> has been proved useful in non-stationary data analysis, but it cannot track very sensitive sudden changes in the time direction and is not well suited to analyze transients. Wavelet analysis has been successfully applied to many applications, such as speech coding and audio signal compression<sup>[3]</sup>, heart sounds analysis and classification<sup>[4-7]</sup>. This is attributed to the fact that wavelets can be natural bases for the representation of some physical signs, particularly non-stationary signals, such as heart sounds, which are often characterized by localization in time.

In wavelet analysis, a prototype basis function called the wavelet mother  $\Psi(t)$  is used. A continuous signal  $x(t)$  is mapped into the time scale domain as<sup>[3]</sup>.

$$WV(a,b) = \frac{1}{\sqrt{a}} \int_{-\infty}^{\infty} x(t) \Psi\left(\frac{t-b}{a}\right) dt \quad (1)$$

The parameter  $a$  is a scaling of the time variable  $t$  and  $b$  is a time shift. The signal  $x(t)$  in Eq. (1) is then decomposed by basis functions obtained by translation and dilation of the mother wavelet  $\Psi(t)$ . Note that for small  $a$  (high frequency), the basis function is compressed and short. Consequently, temporal time information can naturally be captured<sup>[8]</sup>, i.e. high time resolution is attained. When  $a$  is large (low frequency), a dilated basis function that represents low frequency components of the signal results hence providing high resolution in frequency. It is obvious that one key advantage of wavelet analysis is the ability to automatically trade resolution in frequency for resolution in time as the frequency changes from low to high.

In continuous wavelet transform is used to analyze heart sound signals<sup>[4,9]</sup>. In particular, a time-frequency transform of the signal is exploited to identify spectral characteristics of different heart sound signals (of normal and abnormal hearts) depending on time and results were shown to be promising. However, continuous wavelet transform suffers some pitfalls. Signal mapping in Eq. (1) is highly redundant since parameters  $a$  and  $b$  are continuous and hence, the corresponding inverse transform is not unique<sup>[6]</sup>. Though usually the parameters are discretized, redundancy still exists unless a proper discretization is made and the right choice of  $\Psi(t)$  is used.

Equation (1) shows that resolution in time is regularly spread in a logarithmic scale in time. This is inherent in the continuous wavelet transform equation and it is not always possible to change this scheme to meet other resolution requirements. Furthermore, continuous wavelet transform is only suitable for off-line processing. Implementation of Eq. (1) for on-line operation requires huge processing power and is not practical. Therefore, continuous wavelet analysis is of minor practical significance.

In this paper, discrete wavelet and filter banks theory will be used to design and implement a special structure based on the information and characteristics of the heart beat sounds signals and murmurs. Each signal is split into several level bands, where each band can explore certain important information and suppress the surrounding activities that carry different frequency components. This method makes the detection and classification of heart diseases easier, because the heart sound signal under investigation becomes fully exposed in both time and frequency.

### MATERIALS AND METHODS

The introduction of the concept of multi-resolution signal analysis has provided a significant tool to the practical application of wavelet analysis<sup>[10]</sup>. From the multi-resolution theory, a square integrable signal  $x(t)$  can be represented by orthogonal subspaces that are spanned by orthogonal bases of different scales. Accordingly, the signal  $x(t)$  can be viewed in different resolution levels. A square integrable signal  $x(t)$  can be expanded in terms of the translates and dilates of the wavelet  $\Psi(t)$  as<sup>[10]</sup>:

$$x(t) = \sum_i \sum_m 2^{-i/2} \alpha(i, m) \Psi(2^{-i}t - m) \quad (2)$$

Here

$$\alpha(i, m) = 2^{-i/2} \int_{-\infty}^{\infty} x(t) \Psi(2^{-i}t - m) dt \quad (3)$$

and  $i, m, \in \mathbb{Z}$ . Here,  $\mathbb{Z}$  represents a set of integers. From a signal processing point of view, the wavelet  $x(t)$  is a band pass filter with a central frequency  $w_0$ . Eq. (2) shows that the wavelet coefficients  $\alpha(i, m)$  carry information about the signal  $x(t)$  at time instant  $2^i m$  in the proximity of the frequency  $2^{-i} w_0$ .

The wavelet functions  $2^{-i/2} \Psi(2^{-i}t - m)$  constitute orthonormal basis for the subspaces  $W_i$  and the wavelet  $2^{-(i+1)/2} \Psi(2^{-(i+1)}t - m)$  spans the subspaces  $W_{i+1}$ . Note that the function is compressed in time by a factor of 2 relative to the function  $2^{-i/2} \Psi(2^{-i}t - m)$ . As a result, the signal in the space  $W_i$  has double the resolution in time of the

signal in  $W_{i+1}$ . Note also that the subspaces are mutually orthogonal. That removes the redundancy inherently found in continuous wavelet analysis. These subspaces define a multi-resolution analysis of the signal  $x(t)$  where the signal space is represented as a direct sum of various resolutions as follows<sup>[10]</sup>:

$$\begin{aligned} \text{signal space} &= W_i \oplus W_{i+1} \oplus W_{i+2} \oplus \dots \\ &= \oplus W_i \quad (i \in \mathbb{Z}) \end{aligned} \quad (4)$$

It is clear from Eq. (4) that the signal  $x(t)$  can be uniquely expanded into many sub-band signals of different time-frequency resolutions. This constitutes the essence of discrete wavelet analysis.

**Discrete wavelet and filter banks:** Recently, the theory of multi-resolution analysis of signals and filter banks were brought together<sup>[11]</sup>. Based on this relationship, it becomes possible to implement the discrete wavelet expansion in Eq. (2) with very low complexity. It was established that the projection of the signal  $x(t)$  into the subspace  $W_i$  can be achieved by passing the signal through iterated multirate filters. The filter banks system in Fig. 1, realizes the discrete wavelet transform. For example, in the upper branch in Fig. 1, the signal is filtered by  $h_1(n)$  and then sub-sampled by a factor of two. The output of this branch is approximately the wavelet expansion coefficients of the subspace  $W_0$ , i.e.  $\alpha(0, m)$ .

One immediate result from multi-resolution analysis is that the mother wavelet  $\Psi(t)$  can be obtained from a scaling function  $\phi(t)$  as<sup>[12]</sup>:

$$\Psi(t) = \sum_{n=0}^{\infty} h_1(n) \phi(2t - n) \quad (5)$$

The scaling function  $\phi(t)$  satisfies also the equation,

$$\phi(t) = \sum_{n=0}^{\infty} h_0(n) \phi(2t - n) \quad (6)$$

Our purpose is to introduce a computationally efficient implementation of the wavelet expansion for the current application and therefore, infinite length filters  $h_0(n)$  and  $h_1(n)$  associated with infinite length wavelets are of no practical interest. Our concentration will be on compact support (finite)  $\Psi(t)$  that results in finite length filters  $h_0(n)$  and  $h_1(n)$ , i.e.  $0 \leq n \leq L - 1$ . Note from Eq. (6) that the coefficients of the filter  $h_0(n)$  correspond to the expansion coefficients of  $\phi(t)$  in terms of its dilation  $\phi(2t)$ . Thus, discrete wavelet analysis is performed in Fig. 1, without the explicit need of the wavelet mother  $\Psi(t)$  and the scaling function  $\phi(t)$ . Only  $h_0(n)$  is needed to be derived, where  $h_1(n)$  can be found as<sup>[12]</sup>:

$$h_1(n) = (-1)^{L-n-1} h_0(L-n-1), \quad n = 0, 1, \dots, L-1$$

The filter  $h_0(n)$  is a half band low pass filter and then from Eq. (7),  $h_1(n)$  is a half band high pass filter. In addition, for  $h_0(n)$  and  $h_1(n)$  to have suitable expansion coefficients in Eqs. (5) And (6), the following conditions should hold<sup>[12]</sup>:

$$\begin{aligned} \sum_{n=0}^{L-1} h_0(n) &= \sqrt{2}, & \sum_{n=0}^{L-1} h_0^2 &= 1, \\ \sum_{n=0}^{L-1} h_1(n) &= 0, & \sum_{n=0}^{L-1} h_1^2 &= 1, \end{aligned} \quad (7)$$

Practically, the number of iterations of multirate filters in Fig. 1 should be finite. The lower branch in Fig.1 stops after a certain number of iterations with the expectation that the tree structure will best approximate wavelet expansion of the signal in Eq. (2). Consequently,  $h_0(n)$  must be selected such that the system in Fig. 1 converges to Eq. (2) with subsequent filters being scaled versions of each other. This can be achieved if the filter  $h_0(n)$  has a sufficient number of zeros at  $w = \pi$ <sup>[3]</sup>. This provides a regular wavelet and guarantees that the iterates of the filter converge to a continuous function.

**Extension of the tree structure:** We have shown that by iteration of the system in Fig. 1, the system computes the discrete wavelet transform. Note that in this tree structure, we iterate the system on the lower band only, i.e. only the output of the low pass filter  $h_0(n)$  is decomposed further. At the upper branch, the output has a high time resolution while its frequency resolution is low compared to other branches. The signal is projected onto the subspace  $W_0$  which is effectively the subspace of the signals with frequencies in the interval  $[\pi/2, \pi]$ . In our proposed application where heart sound signals are involved, different resolutions are required at different branches. Thus, one needs to adapt this structure to the application to fulfill certain time-frequency necessities in each branch while keeping the full advantages of multi-resolution analysis. The output of the high pass filter can be decomposed further to meet the required resolution in each branch.

The heart sound signals have an effective frequency bandwidth of 600 Hz. as shown in Fig. 2. Objective of present study is to view the heart sound signal in different wavelet subspaces by splitting up the signal with varying resolutions in time and frequency. A 7-level structure is designed and is shown in Fig. 3. The frequency interval (low and high cut off frequencies) of each of the seven levels is shown in this figure in Hz. This structure is based on our experimentations with heart sound signals of normal and abnormal hearts with different diseases. Note that each band in Fig. 3, describes the signal uniquely at the corresponding scale and the

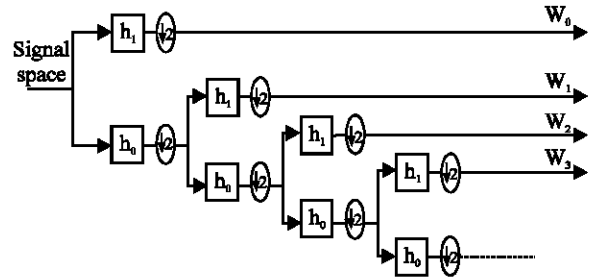


Fig. 1: Wavelet analysis using filter banks with a line structure

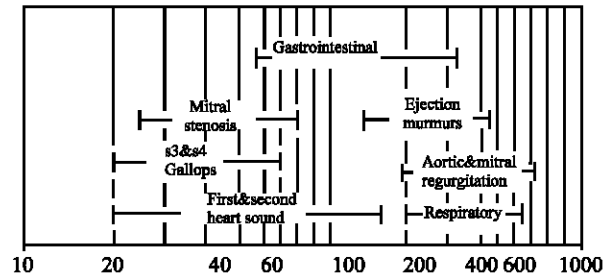


Fig. 2: Heart sound signals frequency band width (Hz)

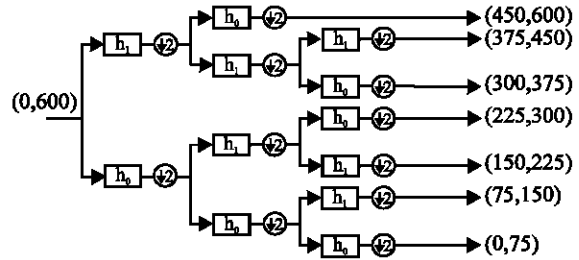


Fig. 3: Wavelet analysis using filter banks with a structure used in heart sounds

attained information is non-overlapping with any from other branches.

Many wavelet mothers with various properties exist. Accordingly, many filters  $h_0(n)$  that exhibit different behaviours are known. One popular group of compact support filters was proposed by Daubechies<sup>[12]</sup>. This class of filters has good resolution both in time and frequency. This group offers different filter orders of  $h_0(n)$ , with the shortest having 4-coefficients. Note that short filters provide high selectivity in time. Daubechies-6 was found to be suitable in this application since it provides good time-frequency characteristics and requires low computational complexity. The coefficients  $h_0(n)$  of this filter are<sup>[7]</sup> equal to:

$$0.332670552950, \quad 0.806891509311, \quad 0.459877502118, \\ -0.135011020010, \quad -0.085441273882 \quad \text{and} \quad 0,035226291882$$

The coefficients  $h_1(n)$  of the associated filter can be easily derived from Eq. (7).

**Hardware system and data collection:** A specially made electronic stethoscope is used by a Cardiologist to detect heart sounds from subjects under clinical examination. The clinical findings are recorded by the cardiologist for further investigation. The heart sound signals were amplified by Gould Universal Signal Conditioner with isolated pre amplifier and adjustable frequency response DC-10KHz. (-6dB) and a measurement range (full scale) 25uV-250 mV. The filter is used to reduce any possible noise due to the measurement system wiring. It also prevents aliasing effect induced by digitization. A sixteen channel twelve bit Metrabyte signal data acquisition board is used to digitize the detected heart sound signal and the ECG waveform at the same time by using two different channels with a 1500 Hz sampling rate. A Dadisp digital signal processing software on a Pentium III computer is used along with the data acquisition board. Real time data of both the PCG signal and the ECG signal were saved and stored for further analysis, processing and investigation.

## RESULTS AND DISCUSSION

In a normal cardiac cycle, there are two major sounds: the first heart sound (S1) followed by a silent systolic pause and the second heart sound (S2) followed by a silent diastolic pause as depicted in Fig. 4a. The output signal of each branch in Fig. 3 has been interpolated to illustrate the characteristics of each individual sub band signal. The output signals of the first five bands are shown respectively in Fig. 4b. In some abnormal cases, a very low frequency third heart sound (S3) may be heard just after (S2). In late diastole, a fourth heart sound (S4) may sometimes be heard. In addition to these sounds, valvular clicks and snaps are occasionally heard. Murmurs, which are caused by certain cardiovascular defects and diseases, may occur during the cardiac cycle. Features of heart sound and murmurs, such as frequencies range, temporal time location and intensity are different from one disease to another<sup>[13]</sup>. Because of this, accurate diagnosis through cardiac auscultation in examination of a patient with complicated murmurs can be difficult for medicine students and many untrained physicians and clinician, because they should be able to distinguish in less than one second all these events in order to give the right diagnosis, such as, distinguishing opening snap from the third heart sound, both located just after the second heart sound S2, or distinguishing the fourth heart sound from the late diastolic murmur just before the first heart sound, or separation between high and low.

Frequency systolic and diastolic murmurs or detecting the auscultatory gap and so on. A few cases

will be presented in this paper to show how easily and effectively this method can overcome the aforementioned difficulties. The heart sound signals of the normal and different abnormal cases and their sub bands outputs are shown in Fig. 4-6, where the normal case and its sub bands output are shown in Fig. 4 and the following abnormal cases: the Atrial septal defect (ASD), the Aortic incompetence (AI), the Mitral incompetence (MI), the Systemic hypertension (SH), the Pulmonary stenosis (PS) and the Ventricular septal defect (VSD) cases are shown in Fig. 5, The subband outputs of the aforementioned cases are shown in Fig. 6,7. It can be seen that for the untrained ear, it is not easy to differentiate, for example, between the normal case shown in Fig. 4 and the Atrial septal defect (ASD) and the Systemic hypertension (SH), both shown in Fig. 5. It is also difficult to differentiate between the Pulmonary stenosis case and the Ventricular septal defect case, or to distinguish between the Mitral incompetence case and the Aortic incompetence case, all shown in Fig. 5. By studying the sub bands outputs of all these cases, it can be seen that each band in each case can reveal very specific details, features and events that characterized that particular case. This makes the distinction between the cases possible.

To elaborate more, the output of one subband is chosen and shown for each case to explore the ability of the proposed technique in distinguishing between normal and abnormal cases as well as between different abnormalities. From a medical point of view, each abnormal case has its own features and events which characterize it. In the following section, six different abnormal cases will be studied; the main features and characteristics of each will be given and compared with the events and features extracted from the sub band outputs shown in Fig. 6-7.

### Case 1: Atrial septal defect (ASD)

This case is characterized mainly by:

- a) The presence of systolic murmurs, which start after the first heart sound (S1) and end before the second heart sound. (S2).
- b) The presence of auscultatory gap
- c) A wide split in the second heart sound components

### Case 2: Aortic incompetence (AI)

This case is mainly characterized by:

- a) The presence of ejection systolic murmurs starting just after the first heart sound (S1) and ends well before the second heart sound.
- b) The presence of soft high pitched decrescendo diastolic murmurs starts immediately after the second heart sound (S2)



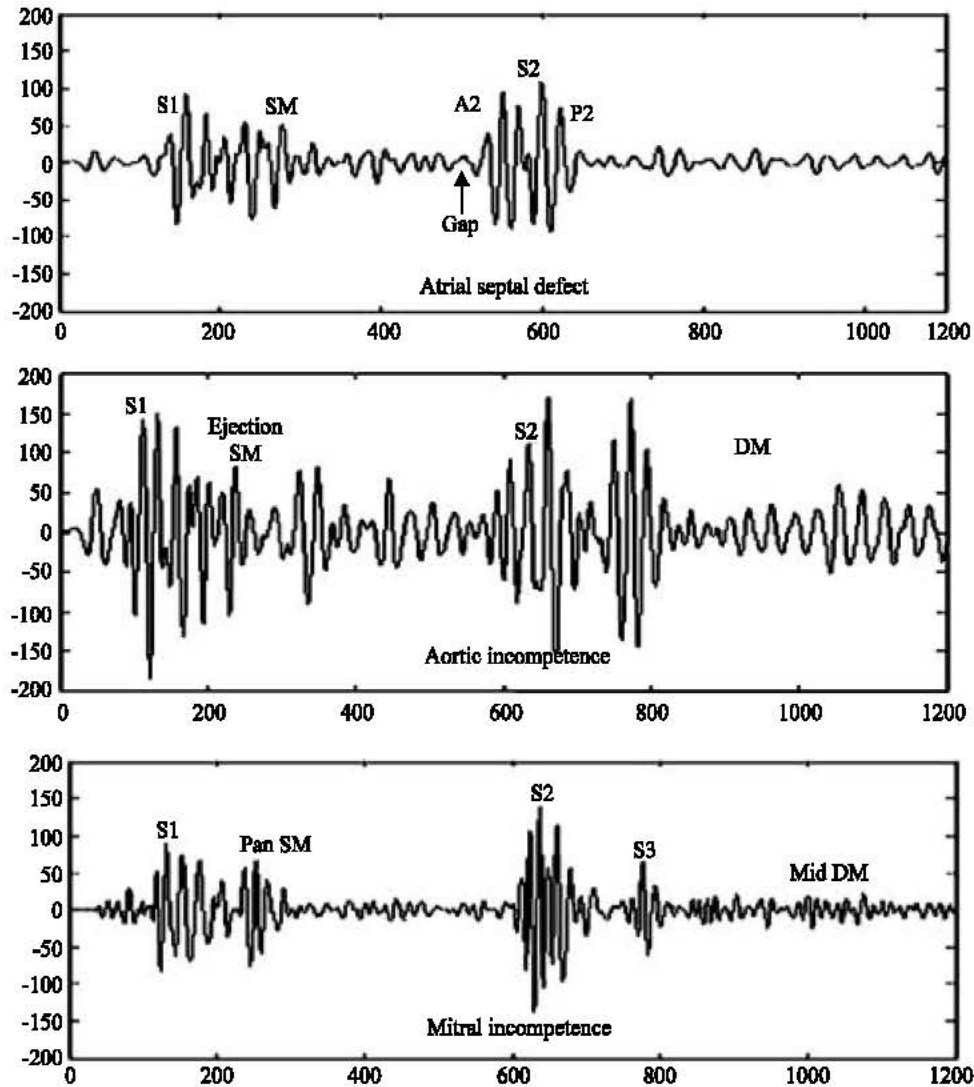


Figure abbreviations: S1 first sound; S2 second sound; S3 third sound, S4 fourth sound; SM systolic murmur; DM diastolic murmur; A2 aortic; P2 pulmonary

Fig. 6: Subbands output waveform of ASD, AI and MI cases shown in Fig. 5

**Case 3: Mitral incompetence (MI)**

This case is mainly characterized by:

- a) The presence of soft high pitched pan systolic murmurs starting just after the first heart Sound (S1).
- b) The presence of short low pitch mid diastolic murmurs beginning right after the third heart Sound
- c) The presence of the third heart sound.

**Case 4: Systemic hypertension (SH)**

This case is characterized mainly by:

- a) The presence of short ejection systolic murmurs.

- b) The presence of the fourth heart sound just before the first heart sound.

**Case 5: Pulmonary stenosis (PS)**

This case is characterized mainly by:

- a) The presence of harsh, long and high pitched frequency systolic murmurs starting with the first heart sound (S1)
- b) Low and soft second heart sound which cannot be heard because of the surrounding murmur
- c) The first heart sound is buried with the associated murmurs.

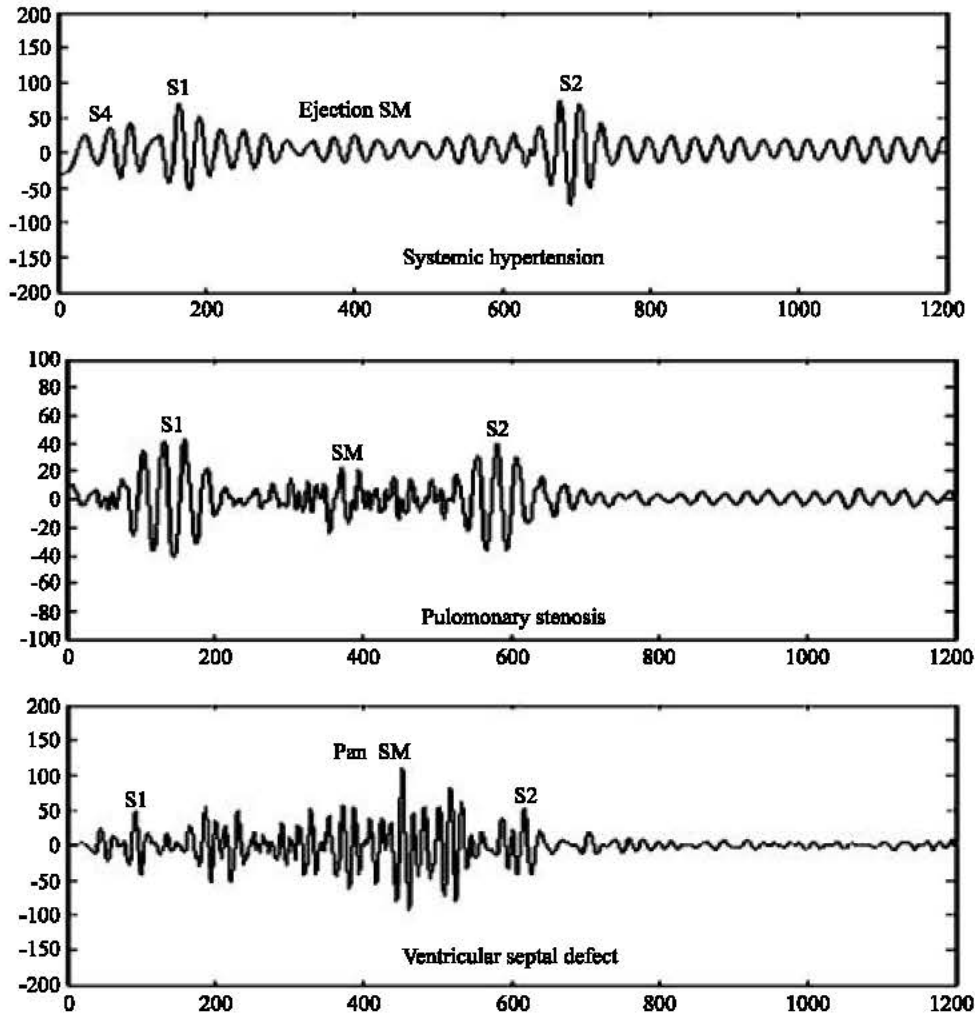


Fig. 7: Subbands output waveform of SH, PS and VSD case shown in Fig. 5

**Case 6: Ventricular septal defect (VSD)**

This case is characterized mainly by:

- a) The presence of rough, high pitched pan systolic murmurs begins with the first heart sound (S1) and extends to cover the second heart sound (S2).
- b) The difficulty of discrimination between both the first and second heart sounds from the murmur.

As mentioned earlier, for the untrained ear it is very difficult to recognize the presence of auscultatory gap and the presence of wide split in the second heart sound components in the ASD case, or to recognize the presence of ejection systolic murmurs starting just after the first heart sound (S1) and ending well before the second heart sound, and the presence of soft high pitched decrescendo diastolic murmurs starts immediately after the second heart sound (S2) in the AI case (Fig. 5).

Also it is not easy to distinguish the first heart sound signal from the pan systolic murmur and to recognize the presence of the faint third heart sound in the MI case, or to distinguish the presence of the fourth heart sound in the SH case. Moreover and because of the harsh systolic murmur, it is very difficult to discern both the first and second heart sounds in the PS case and to discriminate both the first and second heart sounds from the murmurs in the VSD case. The subband outputs of the aforementioned cases are shown in Fig. 6 and 7. The main features and events which characterized each case can be extracted.

In the ASD case, the systolic murmur, the wide split in the second heart sound and the auscultatory gap are recognized. For AI case, the ejection systolic murmur and diastolic murmur are distinguished. In MI case, the pan systolic murmur, the mid diastolic murmur and the faint third heart sound can be extracted without any difficulty.

Also, as shown in Fig. 7, the fourth heart sound and the ejection systolic murmur in the SH case, are discriminated from the first heart sound. In PS case, the buried first heart sound and the low-soft second heart sounds are separated from the harsh high frequency systolic murmur. For VSD case, both the first and second heart sounds are separated from the rough high pitched pan systolic murmur.

Moreover, the discrimination between the seemingly similar heart sounds for the untrained ear, such as the normal heart sound and systemic hypertension or the atrial septal defect and the systemic hypertension, or the aortic incompetence and the mitral incompetence, or the pulmonary stenosis and the ventricular septal defect, can be obtained.

In conclusion, the described method overcomes the aforementioned difficulties and provides vast amount of accurate and meaningful information of great diagnostic assistance. Viewing the heart sound signals in different wavelet subspaces by splitting up each signal into seven levels, as shown in Fig. 3 and choosing the right filter coefficients, a good time-frequency characteristics is obtained. Also, it makes the detection and classification of heart diseases easier. This is because the heart sound signal under study becomes fully exposed in both time and frequency. This means that any events in the cardiac cycle can be detected and classified. We were able to separate the faint third sound from the second heart sound and the diastolic murmur in the mitral incompetence case. Also, the fourth heart sound can be distinguished from the first heart sound in systemic hypertension case. Thirteen different cases were explored using the proposed structure. Preliminary results which show the significance of this technique as an informative educational diagnostic technique tool are believed to be satisfactory and promising and it might help to bring cardiac auscultation into prominence again along with more modern technologies such as scans, echo and Doppler scans.

## REFERENCES

1. Rongayyan, R.M. and R.J. Lehner, 1988. Phonocardiogram signal analysis: a review. *CRC Critical Reviews in Biomedical Engineering*, 15: 211-236.
2. Cohen, L., 1989. Time frequency distribution: a review, *Proc. of the IEEE*, 77: 941-981.
3. Rioul, O. and M. Vetterli, 1991. Wavelets and signal processing. *IEEE SP Magazine*, pp: 14-38.
4. Khadra, L., M. Matalgah, B. El-Asir and S. Mawagdeh, 1991. The wavelet transform and its application to phonocardiogram signal processing. *Med. Informatic*, 16: 271-277.
5. El-Asir, B., L. Khadra, A.H. Abbasi and M.M. Jaffer, 1996. Multiresolution analysis of heart sounds *IEEE ICECS*. Rodos.
6. Debjais, F., L.G. Durand, Z. Ouo and R. Guarlo, 1997. Time-frequency analysis of heart murmurs. Part II: optimization of time- frequency representations and performance evaluation. *Medical and Biological Engineering and Computing*, 35: 480-485.
7. Olmez, T. And Z. Dokur, 2003. Classification of heart sounds using an artificial neural network. *Pattern Recognition Letters*, 24: 617-629.
8. Daubechies, I., 1990. The wavelet transform, time-frequency localization and signal analysis. *IEEE Trans. Inform. Theory*, 36: 961-1005.
9. El-Asir, B., L. Khadra, A.H. Abbasi and M.M. Jaffer, 1996. 'Time frequency analysis of heart sounds' *IEEE TENCON 96 Digital signal processing*. Perth, Australia, pp: 553.
10. Rioul, O., 1993. A Discrete-time multiresolution theory. *IEEE Trans. Signal Processing*, 41: 2591-2606.
11. Evangelista, G., 1989. Orthogonal wavelet transforms and filter banks in *Proc. 23rd Asilomar Conf. Circuits, Systems, Computers*. Pacific Grove, pp: 489.
12. Daubechies, I., 1988. Orthogonal bases of compactly supported wavelets. *Commun. Pure App. Math.*, 41: 909-996.
13. Erickson, B., 1997. *Heart Sounds and Murmurs: A Practical Guid* (3rd Edn). Mosby Year Book, Inc: St. Louis, Missouri.